Phys. Med. Biol. **55** (2010) 615–622 doi:10.1088/0031-9155/55/3/004

In vivo endoscopic multi-beam optical coherence tomography

Beau A Standish[1], Kenneth K C Lee[2], Adrian Mariampillai[1], Nigel R Munce[1], Michael K K Leung[1], Victor X D Yang[2,3,4] and I Alex Vitkin[1,2,5]

[1] Deptartment of Medical Biophysics, University of Toronto, Toronto, Canada
[2] Ontario Cancer Institute/University Health Network, Toronto, Canada
[3] Department of Electrical and Computer Engineering, Ryerson University, Toronto, Canada
[4] Department of Imaging Research, Sunnybrook Health Science Center, Toronto, Canada
[5] Department of Radiation Oncology, University of Toronto, Toronto, Canada

E-mail: standish@ee.ryerson.ca

Received 2 June 2009, in final form 12 November 2009
Published 13 January 2010
Online at stacks.iop.org/PMB/55/615

Abstract
A multichannel optical coherence tomography (multi-beam OCT) system and an *in vivo* endoscopic imaging probe were developed using a swept-source OCT system. The distal optics were micro-machined to produce a high numerical aperture, multi-focus fibre optic array. This combination resulted in a transverse design resolution of <10 μm full width half maximum (FWHM) throughout the entire imaging range, while also increasing the signal intensity within the focus of the individual channels. The system was used in a pre-clinical rabbit study to acquire *in vivo* structural images of the colon and *ex vivo* images of the oesophagus and trachea. A good correlation between the structural multi-beam OCT images and H&E histology was achieved, demonstrating the feasibility of this high-resolution system and its potential for *in vivo* human endoscopic imaging.

(Some figures in this article are in colour only in the electronic version)

Introduction

Optical coherence tomography (OCT) (Huang *et al* 1991, Fujimoto *et al* 2000) is a novel biomedical imaging modality that offers micron resolution of subsurface tissue and has been extended to endoscopic (Yang *et al* 2005, Chen *et al* 2007, Westphal *et al* 2005, Vakoc *et al* 2007) and bronchoscopic (Lam *et al* 2008, Coxson *et al* 2008) imaging scenarios. The distal optics of the endoscopic or bronchoscopic probe are of great importance and require careful design and manufacture, as they directly influence the lateral resolution and the signal intensity within the Raleigh range of an OCT axial scan. High numerical aperture (NA)

optics provide improved resolution but suffer from a shallow depth of field. To overcome this limitation, a time-domain OCT system could use a dynamic focus-tracking system to mechanically synchronize the focus with the movement of the reference mirror using micro-electrical–mechanical-membrane technology (Yang *et al* 2006). If one wants to take advantage of the signal-to-noise and imaging speed of frequency-domain (FD) OCT (Fercher *et al* 2003), one must employ a different technique to achieve high transverse resolution, as the depth information of the entire axial scan is encoded within the captured spectrum and sampled simultaneously. Therefore, we propose a solution that separates the depth of field into sub-fields using a separately focused beam for each of these fields. Previously, we developed a fibre-based multichannel OCT (multi-beam OCT) system comprising a micro-machined array tip, which achieved good lateral resolution while also maintaining a full depth of imaging of $\sim$500 μm (Yang *et al* 2004). In collaboration with Michelson Diagnostics Ltd (Kent, UK), this design was packaged into an OCT scanning system capable of maintaining high transverse resolution, via the use of multiple optical fibre's, throughout the $\sim$2 mm OCT depth of field (Holmes *et al* 2008). Recent improvements in the fabrication of optics offer an opportunity to miniaturize this multi-beam OCT scheme and make it more suitable for non-invasive *in vivo* endoscopic and bronchoscopic applications. In this paper, we describe a miniaturized probe for a multi-beam OCT system capable of acquiring *in vivo* structural images of the gastrointestinal tract of a rabbit, while maintaining high transverse and axial resolution throughout the imaging depth.

Materials and methods

Multi-beam OCT system and imaging probe

The multi-beam FD-OCT system consisted of a conventional Michelson interferometer incorporating a Santec (HSL-2000, Santec, NJ, USA) swept-source laser operating at a central wavelength of 1300 nm with a spectral bandwidth of approximately 100 nm. This resulted in an axial resolution of $\sim$7.4 μm in air or $\sim$5.5 μm in tissue (assume index of tissue to be $n =$ 1.35). The output beam was split into four 'beamlets' ($4 \times 25\%$) prior to the interferometer (figure 1). The beamlets were directed towards the distal end of the imaging probe and used to scan the tissue. Upon the return path from the tissue, the light interfered with the four reference beams and the resultant interference signal was measured by an array of photodiodes. The portions of the reference mirrors in each of the three beams were individually optimized, providing a focal depth of 0.25 mm stepped at a 0.25 mm interval (resulting in a 0.75 mm imaging depth, while maintaining high transverse resolution). The fourth beam was used to generate a balance signal increasing the signal-to-noise ratio (SNR) in the resultant images. The multi-beam OCT probe was translated in a linear fashion for $\sim$3 mm, with each two-dimensional image consisting of 1094 A-scans and 1024 samples per A-scan. The distal optics were translated via a servo motor with encoder feedback, at a scan rate of 4 Hz, such that the pixels (in tissue) represented an isotropic imaging region. Although it proved difficult to obtain absolute sensitivity measurements with our multi-beam probe, it was generally observed that the system consistently produce image sensitivities in excess of 80 dB, based on observed imaging in human skin, human finger nails and agar phantoms.

A micromachined multi-focus fibre-based optical array tip was first introduced by our group to improve the lateral resolution of the OCT system, while maintaining a comparable imaging depth to that of a single channel OCT system (Yang *et al* 2004). A similar principle was employed in this multi-beam OCT system. High numerical aperture lenses (NA = 0.15), at the distal end of each channel, produced an improved lateral resolution but with a smaller

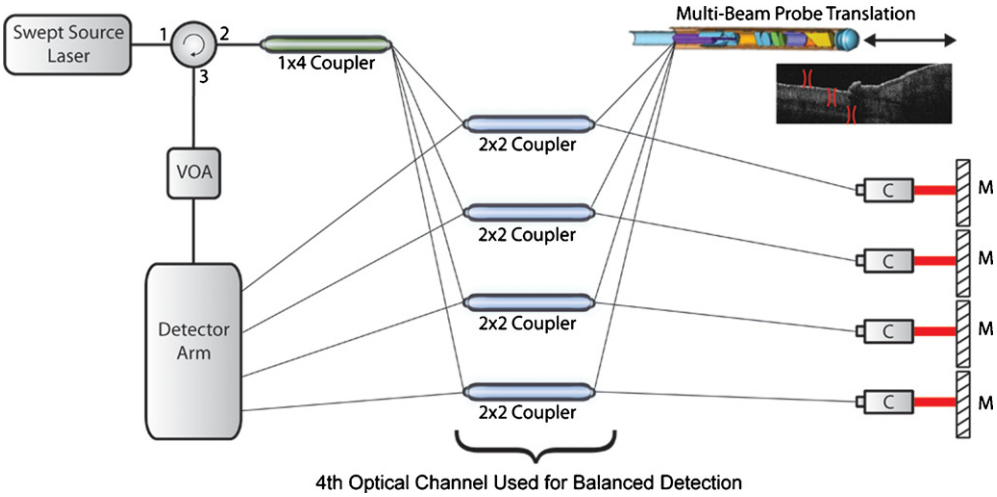

Figure 1. Multi-beam OCT system. The output beam was split into four 'beamlets' (4 × 25%) prior to the interferometer. The beams were directed towards the distal end of the imaging probe, where the three beamlets had a stepped imaging depth of field. Upon the return path from the tissue, the light interfered with the four reference beams and the resultant interference signal was measured by an array of photodiodes. The position of each mirror in the reference arm could be individually optimized, providing a focal depth of 0.25 mm stepped at a 0.25 mm interval (resulting in a 0.75 mm depth of high transverse resolution). The fourth beam was used to generate a balance signal. The multi-beam probe assembly is discussed in detail in figure 2. VOA, variable optical attenuator; C, collimator; M, mirror.

working distance. Therefore, the multi-channel optical array was cascaded such that the individual channels were focused to different depths and through signal processing, stitched together to produce a tiled image. A bulk-optic multi-beam OCT system with the same numerical aperture and beamlet depth spacing, developed by Michelson Diagnostics Ltd, has been shown to resolve 5.5 μm bars on a US Air Force resolution target (Holmes *et al* 2008).

An identical optical arrangement of beams was adopted for the miniature multi-beam fibre optic probe (see figure 2). The mechanical components of the probe assembly were manufactured using conventional turning and milling techniques. The probe tube was machined from a stainless steel hypodermic tube, while the optical spacer rings (used to separate optical components) were turned from brass. The fibre mount was turned from brass with a machined slot (0.5 mm wide by 0.09 mm) into which the fibres were bonded and protected by an outer catheter and inner tube. The lenses were standard catalogue components, which were edged down to fit the diameter of the stainless steel tube. Finally, a mirror was custom made, using standard optical grinding and polishing techniques. With the optical and micromachined components in place, the individual fibres were stripped of their protective sleeving and bonded in place, using a microscope to guide placement. It should be noted that this micromachining and component placement was not a trivial task and required multiple attempts before success.

The selection of optical components for the distal end of the probe consisted of achromatic doublets to limit the effects of chromatic and spherical aberrations of the light exiting the fibres. The details of the lens placement included the first lens being positioned 5.4 mm from the fibre ends with the distance from the second lens to focus being ∼10.8 mm. These lenses were positioned such that the focal range of the first beam was just outside of the catheter

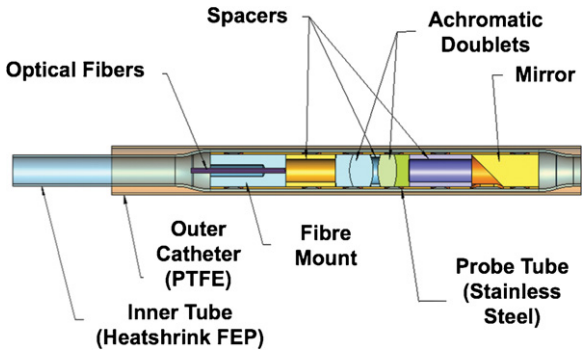

Figure 2. The mechanical components of the probe assembly were manufactured using conventional turning and milling techniques. The probe tube was machined from a stainless steel hypodermic tube, while the optical spacer rings (used to separate optical components) were turned from brass. The fibre mount was turned from brass with a machined slot (0.5 mm wide by 0.09 mm) into which the fibres were bonded and protected by an outer catheter and inner tube. The lenses were standard catalogue components, which were edged down to fit within the stainless steel tube housing. The beam directing mirror was custom made, using standard optical grinding and polishing techniques. PTFE, polytetrafluoroethylene; FEP, fluorinated ethylene propylene.

wall. These parameters resulted in the depth of focus (the Rayleigh range) for each beam to be ∼0.25 mm in tissue (assume refractive index $n = 1.35$ mm), with the first spot being 0.125 mm from the surface of the outer sheath, giving a total 0.75 mm imaging depth for the three spots. The length of the rigid section of the assembly was approx. 40 mm, with the exit window centred at 5.5 mm from the distal end. A mechanical schematic of the probe is demonstrated in figure 3(a). The probe tube was covered in heat shrink fluorinated ethylene propylene tubing, which extended to the proximal drive unit and also served to propel the probe within the outer polytetrafluoroethylene sleeve. The beams were projected through the walls of both plastic tubes via a mirror angled at 55° rather than 45°, to reduce the effect of back reflections. The beam-directing mirror was very slightly curved to correct for minor astigmatism introduced by the cylindrical plastic sleeves. The spot size for each beam was <10 μm FWHM (diffraction limited). To create the stepped focal regions, the four fibres were bonded into the fibre mount (figure 3(b)) with the axial spacing between the fibres set at 250 μm, while the transverse spacing was defined (0.125 mm) by butting the fibres against each other. The final fabricated multi-beam probe had an outside diameter of 5.6 mm (figure 3(c)). Although a direct comparison/contrast of our multi-beam probe to that of a single-beam endoscopic probe, with similar engineering characteristics (i.e. beam focus over 1 mm) would be useful, this was not possible due available resources. However, it was observed that when comparing the individual channels of the multi-beam probe to the overall combined mosaic image, both the signal and image detail dropped off dramatically outside the focal range within the single channel image.

Ex vivo and in vivo imaging

This study used rabbits housed in standard conditions under a protocol approved by the Animal Care Committee of University Health Network, Toronto. Rabbits were anaesthetized via inhalation of an isoflurane/oxygen mixture (2–4% isoflurane) with a nose cone. The lubricated multi-beam OCT imaging probe was inserted into the colon via the rectum. The OCT imaging sessions lasted for approximately 40 min, in parallel with x-ray fluoroscopy for

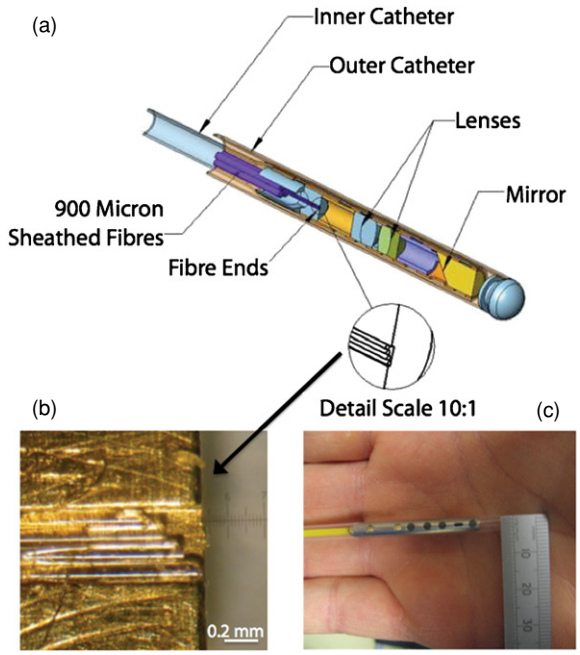

Figure 3. Distal optics of the multi-beam OCT endoscopic probe. (a) Opto-mechanical arrangement of the OCT probe, with inset showing fibre array mounting. The probe was covered in heat shrink fluorinated ethylene propylene tubing, which extended to the proximal drive unit and also serves to propel the probe within the outer catheter. The four fibres were protected within a 900 μm sheathed fibre assembly and the exiting light was collimated. The beams were then projected through the walls of both plastic tubes via a mirror angled at 55°. (b). Close-up of the fibre optics mounted in the brass ferrule, showing stepped arrangement. (c) Outside diameter of the multi-beam OCT probe was 5.6 mm. Scale bar = 0.2 mm.

probe guidance and location. Animals were euthanized (while under isoflurane sedation) via a 1 ml intra-venous injection of euthanyl. The colon and rectum were resected and fixed in a 10% formalin solution for haematoxylin and eosin (H&E) histology comparison. It proved challenging to image the trachea and oesophagus *in vivo,* as the anaesthetic was administered via nose cone, limiting access to the oral cavities under sedation. Therefore, the trachea and oesophagus tissues were resected for *ex vivo* imaging. Following multi-beam OCT imaging, these tissues were also fixed in the 10% formalin solution and processed for H&E histological comparison.

Signal processing and image reconstruction

A LabVIEW program (developed at Michelson Diagnostics Ltd, Kent, UK) was used for real-time data acquisition, image processing and display. The in-focus regions from each channel were segmented from each respective image and combined to create one mosaic image with a high transverse resolution throughout the full depth, as demonstrated in figure 4. The image boundaries were matched through a calibration procedure that involved imaging a phantom consisting of a plastic screw embedded in agarose gel. This calibration procedure aligned the diagonal surfaces of the screw threads in all channels such that the individual channels could be displayed as a continuous mosaic image.

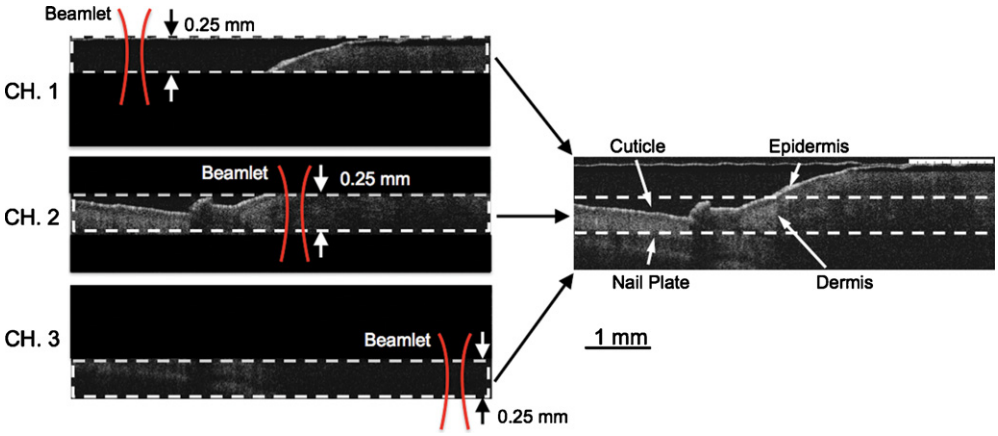

Figure 4. Multi-beam OCT image of a human nail root. Left side displays three separate images acquired simultaneously from the multi-beam OCT probe, where each channel was focused at a different depth (0.25 mm increments in tissue). The right-side image is a mosaic of all three channels, maintaining a high transverse resolution throughout the depth of image. The scale bar of 1 mm applies to all images.

Results and discussions

The multi-beam OCT system imaged the oesophagus (figure 5(a)), trachea (figure 5(b)) and the colon (figure 5(c)), with the epithelial layers being clearly identified. In all of these tissue types, features visible on the multi-beam OCT images corresponded to the epithelial layers identified by histology. In the mosaic images, discontinuities could be seen as a result of the tiling of individual caused by variations in the SNR of individual channels. This discrepancy in SNR throughout the three channels may be related to the limited optical power used to image the tissue. Although the output of the Santec source was approximately 10 mW, the optical power in each of the channels was < 0.7 mW. The SNR may be improved if the light power in each of the optical channels was higher. This may be accomplished either using a source with higher optical output, or by improving coupling efficiency throughout the multi-channel system. As this was a prototype system, all optical connections were implemented using FC connectors. In the future, these connections will be replaced by fusion splicing the fibres throughout the system and this should result in an increase in the optical output power. An alternate approach to improving the SNR would be to implement speckle reduction (Holmes and Hattersley, 2009) and/or to increase the intensity of the sub-beams in the channels that image deeper tissues by use of a non-symmetric optical coupler. For example, in this setup we used a 1 to 4 (25% per channel) optical coupler. If we replaced this with a 1 to 4 (40%, 30%, 20%, 10% per channel) optical coupler, the beams which image the deeper tissue would receive a higher optical power and therefore an improved SNR.

Future technical development includes further miniaturization of the multi-beam probe to a dimension of $\sim$2 mm, which would be suitable for endoscopic use in clinical applications such as intra-operative assessment of oesophageal, oral cancers, colorectal cancers and pre-cancers. Further development is also required to automate the image mosaic process such that the high transverse resolution regions, from each optical channel, are segmented and recombined to produce a final image with minimal user input.

In summary, we have reported a micro-machined multi-focus fibre optic array multi-beam OCT system with improved lateral resolution and a miniature catheterized probe housing,

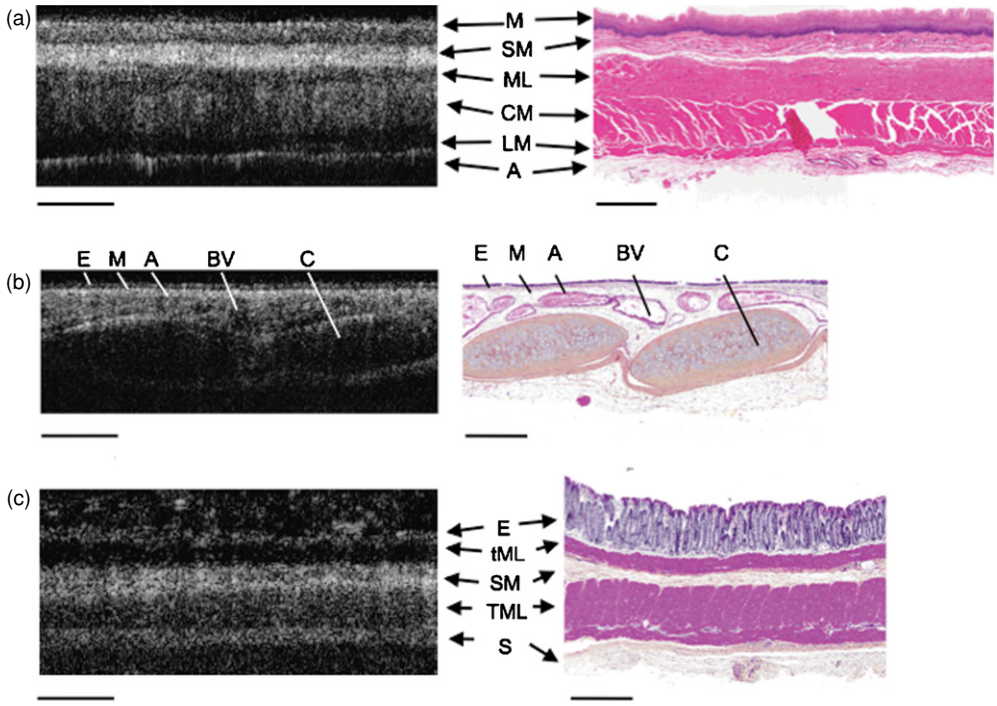

Figure 5. Multi-beam OCT images of rabbit oesophagus, trachea and colon. (a) *Ex vivo* MOCT and H&E histology comparison showing the oesophageal layers: M, mocusa; SM, submocusa; ML, muscularis; CM, circular muscle; LM, longitudinal muscle; A, adventitia. (b) *Ex vivo* multi-beam OCT and H&E histology comparison showing the tracheal layers: E, epithelium; M, mocosa; A, adventitia; BV, blood vessel; C, cartilage. (c) *In vivo* multi-beam OCT and H&E histology comparison showing the different layers of the colon wall: E, epithelium; tML, thin muscle layer; SM, submucosa; TML, thick muscle layer; S, serosa. All scale bars = 500 μm.

and have demonstrated its biological imaging potential in both *ex vivo* and *in vivo* imaging scenarios. With further miniaturization, this system may be suitable for endoscopic and/or bronchoscopic imaging applications to further the pursuit of a non-invasive optical biopsy technique or a device to imaging the response of targeted endoscopic therapy (Standish *et al* 2007).

Acknowledgments

This work was supported by the Canadian Cancer Society through a grant from the National Cancer Institute of Canada and the Canadian Institutes of Health Research. Michelson Diagnostics Ltd (Kent, UK) kindly provided the engineering and financial resources to develop and build the multi-beam OCT probe and processing system.

References

Chen Y *et al* 2007 Ultrahigh resolution optical coherence tomography of Barrett's esophagus: preliminary descriptive clinical study correlating images with histology *Endoscopy* **39** 599–605

Coxson H O, Quiney B, Sin D D, Xing L, McWilliams A M, Mayo J R and Lam S 2008 Airway wall thickness assessed using computed tomography and optical coherence tomography *Am. J. Respir. Crit. Care Med.* **177** 1201–6

Fercher A F, Drexler W, Hitzenberger C K and Lasser T 2003 Optical coherence tomography—principles and applications *Rep. Prog. Phys.* **66** 239–303

Fujimoto J G, Pitris C, Boppart S A and Brezinski M E 2000 Optical coherence tomography: an emerging technology for biomedical imaging and optical biopsy *Neoplasia* **2** 9–25

Holmes J and Hattersley S 2009 Image blending and speckle noise reduction in multi-beam OCT *Proc. SPIE* **7168** 71681N

Holmes J, Hattersley S, Stone N, Bazant-Hegemark F and Barr H 2008 Multi-channel Fourier domain OCT system with superior lateral resolution for biomedical applications *Proc. SPIE* **6847** 684700

Huang D *et al* 1991 Optical coherence tomography *Science* **254** 1178–81

Lam S, Standish B, Baldwin C, McWilliams A, LeRiche J, Gazdar A, Vitkin A I, Yang V, Ikeda N and MacAulay C 2008 *In vivo* optical coherence tomography imaging of preinvasive bronchial lesions *Clin. Cancer Res.* **14** 2006–11

Standish B A, Yang V X D, Munce N R, Wong Kee Song L M, Gardiner G, Lin A, Mao Y I, Vitkin A, Marcon N E and Wilson B C 2007 Doppler optical coherence tomography monitoring of microvascular tissue response during photodynamic therapy in an animal model of Barrett's esophagus *Gastrointest. Endosc.* **66** 326–33

Vakoc B J, Shishko M, Yun S H, Oh W Y, Suter M J, Desjardins A E, Evans J A, Nishioka N S, Tearney G J and Bouma B E 2007 Comprehensive esophageal microscopy by using optical frequency-domain imaging (with video) *Gastrointest. Endosc.* **65** 898–905

Westphal V, Rollins A M, Willis J, Sivak M V Jr and Izatt J A 2005 Correlation of endoscopic optical coherence tomography with histology in the lower-GI tract *Gastrointest. Endosc.* **61** 537–46

Yang V X D, Mao Y, Standish B A, Munce N R, Chiu S, Burnes D, Wilson B C, Alex Vitkin I, Himmer P A and Dickensheets D L 2006 Doppler optical coherence tomography with a micro-electro-mechanical membrane mirror for high-speed dynamic focus tracking *Opt. Lett.* **31** 1262–4

Yang V X D, Munce N, Pekar J, Gordon M L, Lo S, Marcon N E, Wilson B C and Vitkin I A 2004 Micromachined array tip for multifocus fiber-based optical coherence tomography *Opt. Lett.* **29** 1754–6

Yang V X D *et al* 2005 Endoscopic Doppler optical coherence tomography in the human GI tract: initial experience *Gastrointest. Endosc.* **61** 879–90